International Journal of Automotive Technology, Vol. 14, No. 4, pp. 587–594 (2013)
DOI 10.1007/s12239–013–0063–6

pISSN 1229–9138/ eISSN 1976–3832

VIBRATION PATH ANALYSIS AND OPTIMAL DESIGN OF THE SUSPENSION FOR BRAKE JUDDER REDUCTION

K. S. SIM[1)], J. H. LEE[1)], T. W. PARK[2)*] and M. H. CHO[3)]

[1)]Graduate School of Mechanical Engineering, Ajou University, Gyeonggi 443-749, Korea
[2)]Department of Mechanical Engineering, Ajou University, Gyeonggi 443-749, Korea
[3)]Brake System Engineering Team, Hyundai Mobis Co., Ltd., 80-9 Mabuk-dong, Gigeung-gu, Yongin-si, Gyeonggi 446-912, Korea

(Received 28 February 2012; Revised 20 November 2012; Accepted 10 January 2013)

ABSTRACT–Brake judder is abnormal vibration, which is mainly generated by uneven contact between the brake disc and pad. The abnormal vibration from BTV (Brake Torque Variation) is transferred to the suspension and the steering system during braking. In this paper, judder simulation is carried out using a multi-body dynamic analysis program to analyze the relationship between judder and the transfer mechanism, which consists of the suspension and the steering system. In order to verify the analytical model, test results are compared with the simulation results. A sensitivity analysis is also carried out. In addition, an optimization method is presented for judder reduction, using the design of experiments.

KEY WORDS : Brake judder, BTV (Brake Torque Variation), Multi-body dynamic analysis, Design of experiment, Optimization

1. INTRODUCTION

Brake judder is a low-frequency vibration, which is generated by the disturbance due to DTV (Disc Thickness Variation) and BTV (Brake Torque Variation) during high-speed braking. The vibration transferred to the steering wheel makes the driver uncomfortable, and some problems in the stability of the steering system occur. Also, the driver experiences judder as vibrations on the brake pedal, steering wheel, and chassis.

Brake judder is implemented through temperature, frictional, and mechanical effects. An actual vehicle test has been conducted for comparing the characteristics of brake judder (Zhang *et al*., 2007). Generally, there are two main types of brake judder: hot judder and cold judder.

Hot judder is usually caused by thermal and chemical effects, while cold judder is mainly related to disc run-out and DTV (Vries and Wagner, 1992; Haigh *et al*., 1993). Judder caused by disc deformation has been investigated, and optimal design of the disc shape for vibration reduction techniques has been studied. The quality for brake judder is improved by using an optimization methodology (Shin *et al*., 2000; Kim *et al*., 2003).

The relationship between heat deformation and brake cooling performance has been analyzed for the disc shape. Cooling system technology for the disc has been developed for disc performance (Choi *et al*., 2007; Pevec *et al*., 2012). Also, the brake corner system to reduce BTV in the brake judder problem has been studied. A numerical model for determining BTV was constructed using the multi-body dynamics model (Kim *et al*., 2008).

To investigate the vibration pathway of brake judder, low frequency vibration modes of the chassis have been analyzed in several vibration modes during braking. Also, sensitivity analysis regarding judder improvement has been presented through an analysis of the system mode (Hwang and Park, 2005). The vibration mode and bush sensitivity analysis were considered by creating models for judder analysis and judder reduction (Singh and Lukianov, 2007; Meyer, 2005).

Many studies for judder reduction of the brake system have investigated the brake itself. However, studies of the vibration pathway of the brake judder problem are few. Moreover, most of these studies have been limited experimentally. In order to isolate the judder phenomenon from the brake, an efficiency model of the transfer system from judder is needed.

In this study, the full vehicle is modeled by a multi-body dynamic analysis program. Critical parts, such as the steering gear box, bushing, and damper, are modeled for characteristic analysis of judder vibration. The judder transfer system is analyzed by abnormal vibration and sinusoidal brake torque on the front wheel. Also, the analysis results are compared with test results. The verified vehicle model can be used to analyze the judder transfer

**Corresponding author.* e-mail: park@ajou.ac.kr

system. Sensitivity analysis is carried out on components that are connected to the suspension. Judder characteristics are compared with the connected components of the suspension and the steering system. The values of the design variables at the components are presented through an experimental design method for reducing vibration.

The paper is organized as follows: in Section 2 modeling of a multi-body dynamic vehicle is presented, and connection parts, which are the steering gear box, bushing, damper etc., are presented for characteristic analysis of judder vibration. In Section 3, the process of the simulation is presented, and the results of the simulation are compared with the test results. In Section 4, through addressing the vibration path of the suspension, sensitivity analysis and process of optimization are presented using the design of experiment. A comparison of the test result and the proposed optimization process result is presented and discussed in Section 5.

2. MULTI-BODY DYNAMIC VEHICLE MODEL

2.1. Vehicle Modeling

Numerical simulations of a full dynamic vehicle are implemented in commercial multi-body software (MSC Adams/view). The full dynamic vehicle consists of the front suspension, rear suspension, steering system, and tires, as shown in Figure 1. Constraining parts, such as bushings and dampers, are applied using actual vehicle design parameters. The front suspension is modeled as a McPherson strut type, and the rear suspension is modeled as a CTBA (Coupled Torsion Beam Axle). The steering system is modeled with torsion bar compliance and gear clearance. The vibration pathway, which consists of the suspension and steering system, is defined by the overall model. Also, a tire model is applied using Pacejka tire. The overall model is considered with respect to rigid structure.

2.2. Bushing Modeling

In order to simulate brake judder and transfer system relations, a nonlinear bushing is applied, using bush test results. Generally, bushing characteristics are applied for three major aspects, namely, nonlinear static stiffness, frequency-dependent dynamic stiffness, and hysteretic behavior characteristics. The measurement of viscoelastic behavior can be undertaken through static and dynamic methods. In this study, bushing characteristics are measured using a single acting (one-axis) endurance tester.

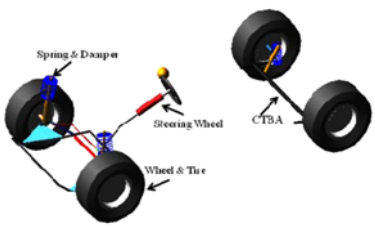

Figure 1. Multi-body dynamic model of the full vehicle.

In order to conduct analysis of the vehicle dynamics, the Kelvin-Voigt bushing model is widely used. but hysteretic characteristic cannot be generated by using the Kelvin-Voigt model. However, the Bouc-Wen model has the advantage of generating the hysteretic characteristic of bushing. Therefore, in the vehicle model, hysteresis behavior is modeled by the Bouc-Wen model through experimental data, using a static test. This system is considered by equation of motion of a single degree of freedom, as follows:

$$m\ddot{x}(t)+c\dot{x}(t)+\Phi(t)=f(t) \tag{1}$$

In the above equation, m is the mass, c is the damping coefficient, x(t) is the displacement, Φ(t) is the restoring force, and f(t) is the exciting force, while the overdot denotes the derivative with respect to time.

It is possible to generate a variety of hyteresis curves by selecting the parameters properly. According to the Bouc-Wen model, the restoring force and displacement are assumed to be described in terms of following the nonlinear differential equation (Ok *et al*., 2005):

$$\Phi(t)=\alpha k x(t)+(1-\alpha)kz(t) \tag{2}$$

$$\dot{z}(t)=A\dot{x}(t)-\beta|\dot{x}(t)||z(t)|^{n-1}z(t)-\gamma\dot{x}(t)|z(t)|^{n} \tag{3}$$

where k is the stiffness, α is the ratio of post-yield stiffenss to pre-yield stiffness, and z(t) is hysteretic displacement. The hyteretic displacement is affected by the parameters (A, β, γ and n are dimensionless quantities controlling the behavior of the model). The physical meaning of the parameters is presented in reference (Ikhouance *et al*., 2007).

The hysteretic behavior test results and simulation results are shown in Figure 2.

Also, the frequency-dependent dynamic stiffness is modeled through experimental data using a dynamic test. The frequency-dependency as a time function of the strain, which is a harmonic function of the frequency, ω, is as follows:

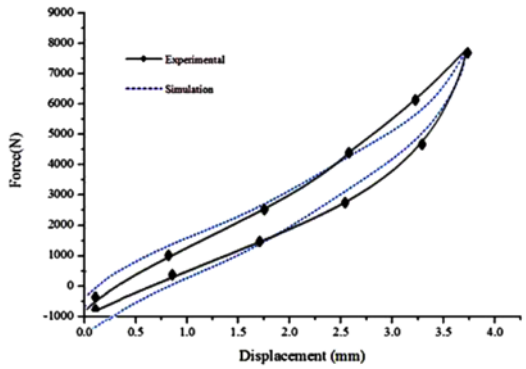

Figure 2. Hysteresis characteristic of the bushing test.

Table 1. Test conditions for the frequency-dependent dynamic stiffness.

Strain, $\gamma(t)$	Frequency, f(Hz)	Initial condition, γ_o (mm)
$\gamma_0 \sin(2\pi\omega t)$	1, 10, 20, 30, 40, 50	0.1, 1.0, 2.0

$$\gamma(t) = \gamma_0 \sin\omega t \tag{4}$$

Tests were carried out to determine the frequency dependent characteristics of the bushing, and the test conditions and parameters are shown in Table 1.

The steady state response of the stress ($\sigma(t)$) is given as Equation (5) (Cho, 2008).

$$\sigma(t) = G'(\omega)\gamma(t) + \frac{G''(\omega)}{\omega}\dot{\gamma}(t) \tag{5}$$

In Equation (5), $\dot{\gamma}(t)$ is the strain velocity, which is the differential of the strain $\gamma(t)$ with respect to time; $G'(\omega)$ is the storage modulus of an elastic material, and $G''(\omega)$ is the loss modulus of a viscous material.

Considering the effects of low frequency, the bushing is tested at less than 50 Hz. The experimental data are applied to the transfer function. Single input and single output transfer functions are expressed in the form of Equation (6).

$$K(s) = \frac{Y(s)}{U(s)} = \frac{a_0 + a_1 s + \ldots + a_{n-1}s^{n-1} + a_n s^n}{b_0 + b_1 s + \ldots + b_{m-1}s^{m-1} + b_m s^m} \tag{6}$$

In the above, s is the Laplace operator, and a_i, b_i are constants.

The main purpose of this study is low-frequency domain analysis of the judder phenomenon. Therefore, the considered frequencies are less than 50 Hz. Only a first-order transfer function should be considered; see Equation (7).

$$K(s) = \frac{Y(s)}{U(s)} = \frac{a_0 + a_1 s}{b_0 + b_1 s} \tag{7}$$

The frequency-dependent dynamic characteristic is shown in Figure 3.

The location of the nonlinear bushing model is described as

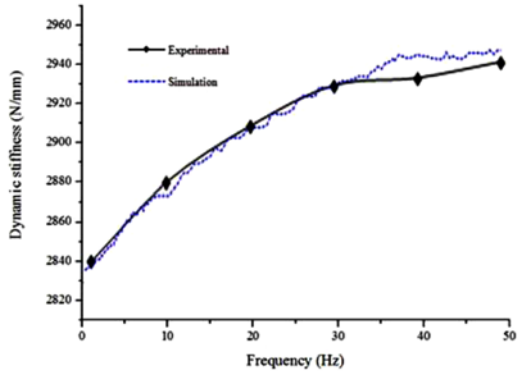

Figure 3. Frequency-dependent dynamic characteristic.

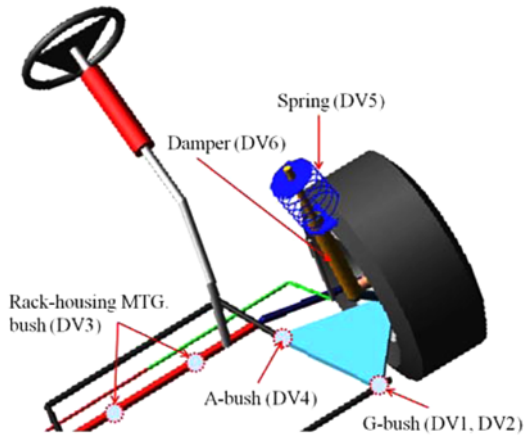

Figure 4. Location of nonlinear bush at front suspension.

shown in Figure 4. Frequency-dependent dynamic stiffness and hysteretic behavior characteristics are considered in G-bush. Also, the A-bush and rack-housing MTG bush are assumed to have nonlinear static stiffness, which is curve fitting data of the hysteric curve of a bush. Other connected bushes are assumed by the linear spring-damper model (6-DOF).

2.3. Damper Modeling

In a vehicle, a damper is a device that decreases the vibrations and oscillations of a vehicle, leading to improved ride quality and increase in comfort. The piston and cylinder serve the damping motion in relative motion. A shock absorber is applied to the damper model, which is expressed as a function of the speed and the load. The experimental data are applied to a spline curve. The damper extension velocity and the compressive velocity are expressed in Equation (8) (Dixon, 1999).

$$V_E = \frac{dL}{dT}, \quad V_C = \frac{dL}{dT} \tag{8}$$

In Equation (8), V_E is the damper extension velocity, and V_C is the compression velocity. L is the length between mounts of the upper and lower ends of the damper, and T is the operating time of the damper.

The front and rear dampers of the multi-body dynamic model are considered by the real damping characteristic of a test car. Also, the spring model is assumed to have linear stiffness. The front damping characteristic of the analysis model is shown in Figure. 5.

2.4. Gear Modeling

The backlash can be classified as hard (i.e. non-differentiable) and dynamic nonlinearity (Voros, 2010).

The judder vibration passes through the rack-pinion gear box; so, the gear behavior is implemented in the backlash. Also, considering the rack-pinion gear constraint, the gear clearance and steering system are mutually applied.

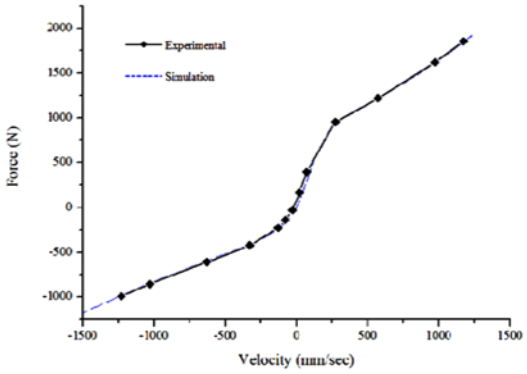

Figure 5. Comparison of the damper test and simulation.

The angular displacement of a pinion gear is expressed by translational displacement of the rack gear, and backlash between the gear teeth.

$$R_p\theta_{sw} = L_r - d/2 \tag{9}$$

where R_p is the radius of a pinion gear, θ_{sw} is the angular displacement of a pinion gear, L_r is the translational displacement of rack gear, and d is the distance beween rack and pinion gear tooth (backlash). Initially, the first gear is placed in the center of the empty space between two teeth of the second gear at the starting point, as shown in Figure 6.

In this paper, the gear-teeth reaction force, F is composed of two nonlinear components: the elastic force, F_k, and the damping force, F_c. Contact will occur when gears traverse the backlash space, as in Equation (10) (Kalantari and Foomani, 2009).

$$|dX| = |R_p\theta_{sw} - L_r| \geq d/2 \tag{10}$$

The left hand side of Equation (10) can be expressed by the distance of the rack-pinion gear. Also, the relationship between elastic force and relative distance (dx) of the gear teeth is shown in Figure 7.

The elastic force of Figure 7 can be described in the following equation:

$$F_k = K \times \left(\frac{dx}{d/2}\right)^n \tag{11}$$

where K is the elastic coefficient, and n is a constant, which affects the rate of increasing F when the gear teeth contact. The nonlinear equation of damping force can be described in the equation:

Table 2. Parameters of the rack-pinion gear model.

Elastic coefficient	Damping coefficient	Backlash	Radius of pitch circle
100 N/m	20 Ns/m	0.25 mm	16.606 mm

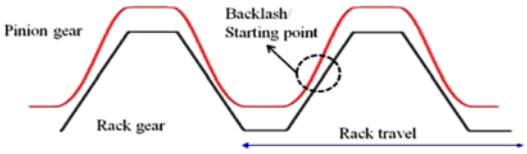

Figure 6. Backlash and starting point of a rack-pinion gear model.

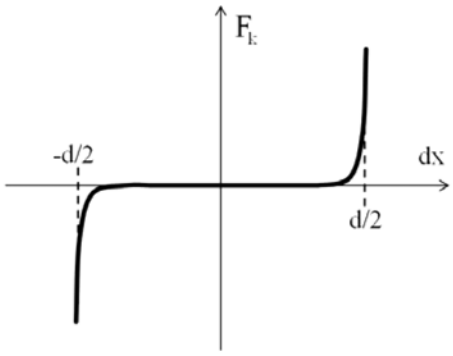

Figure 7. Relastionship between nonlinear elastic force and backlash displacement (Kalantari and Foomani, 2009).

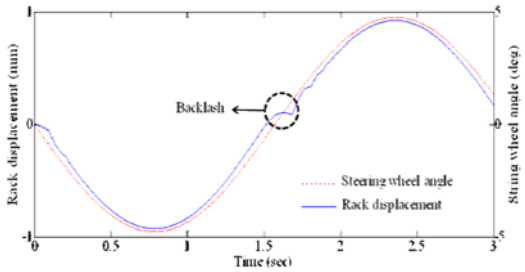

Figure 8. Rack displacement vs. steering wheel angle.

$$F_C = C \times dV \times \left(\frac{dx}{d/2}\right)^{n+1} \tag{12}$$

where C is the damping coefficient, and dV is the difference between the rack-pinion gear velocities. Therefore, the reaction force F is defined as follows:

$$F = F_k + F_c = K \times \left(\frac{dx}{d/2}\right)^n + C \times dV \times \left(\frac{dx}{d/2}\right)^{n+1} \tag{13}$$

The applied backlash characteristic in the model is shown in Figure. 8, and the mathematical model is given by a contact formula as Equation (13).

The rack and pinion gear behavior is expressed by the part of parameters in Table 2.

3. JUDDER SIMULATION

3.1. Measurement

An actual vehicle test is carried out for judder analysis. The

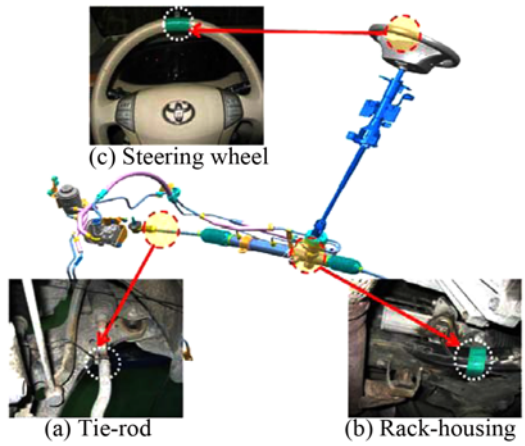

Figure 9. Location of the sensors.

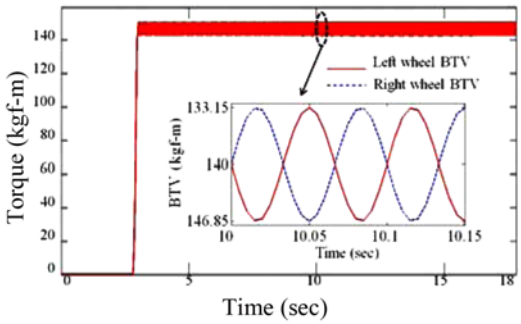

Figure 10. Brake torque and BTV of the simulated excitation on the front wheels.

goal of the vehicle test is to understand the vibration of each part, such as the steering wheel, tie-rod, and rack-housing transfer path. Therefore, an acceleration sensor is attached to each part, as shown in Figure 9. The test is carried out under combined driving conditions, including a vehicle speed range from 180km/h to 70km/h, at a brake deceleration of 0.2Gs in the time domain.

3.2. Simulation Results

A corresponding overall vehicle model based on the test vehicle was applied in the simulation. The brake judder is described by assuming brake torque variation on the wheel. The braking torque is assumed as the sum of a constant torque and the BTV (Meyer, 2005).

$$M_b = M_o + M_{btv} \tag{14}$$

$$M_{btv} = \Delta M_{btv} \sin(\omega t) \tag{15}$$

In the above, M_o is the constant torque and M_{btv} is the BTV, which is the excitation torque of the brake judder. The value of the constant torque is 140 kgf-m, and the value of the BTV is 13.7 kgf-m, as shown in Figure 10, which shows the exciting source of the brake. Also, BTV is

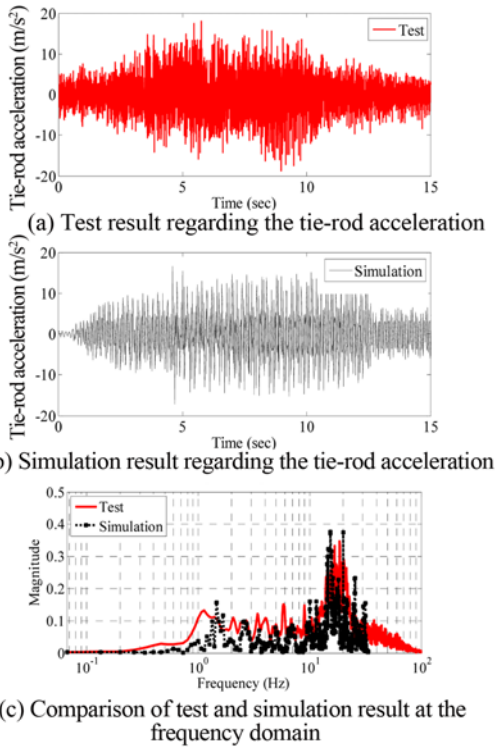

Figure 11. Comparison of the results regarding the tie-rod acceleration.

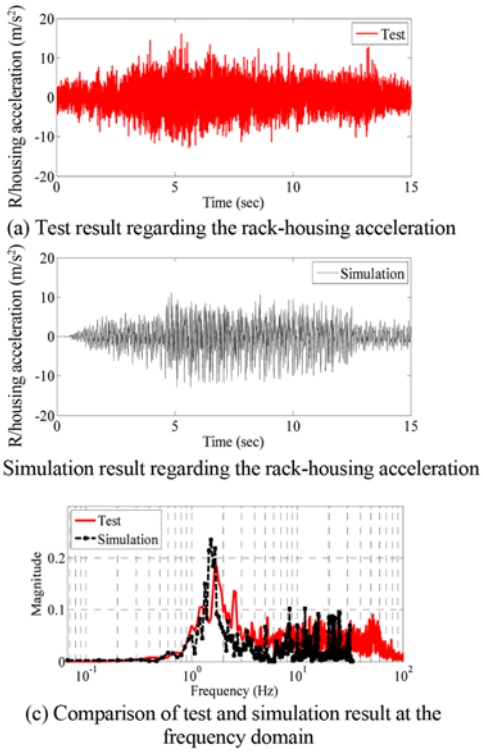

Figure 12. Comparison of the results regarding the rack-housing acceleration.

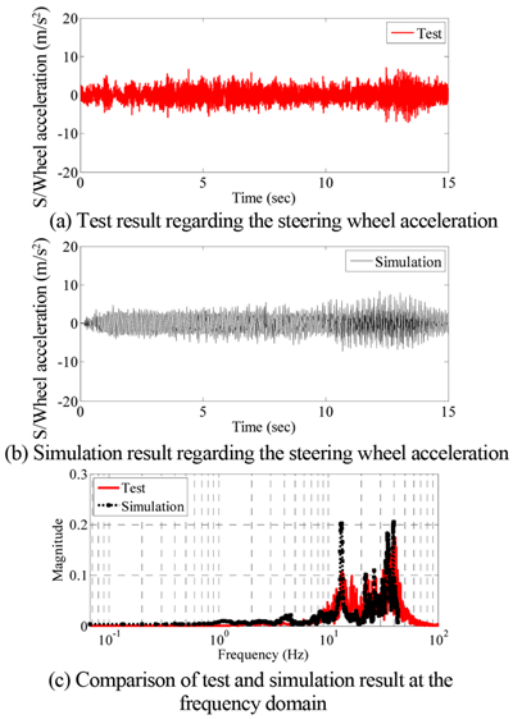

Figure 13. Comparison of the results regarding the steering wheel acceleration.

Table 3. Specification range of 2 level.

Factor (Design variable)			Level	
			-1	+1
Hardness of G-bush (HS)		DV1	60	70
Connected angle of G-bush (deg)		DV2	20	40
Hardness of Rack-housing MTG. Bush (HS)		DV3	70	90
Hardness of A-bush (HS)		DV4	65	75
Stiffness of the spring (kgf/mm)		DV5	2.25	2.75
Damper Characteristic (kNs/m)	Extension	DV6	1.49	1.82
	Compression		0.74	0.90

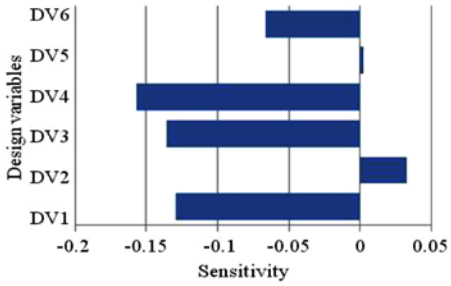

Figure 14. Results of sensitivity analysis.

assumed as a sinusoidal wave on the front/rear wheels, and the judder excitation phase of the right wheel is opposite to the left wheel (180 deg phase shift). Braking torque is applied to all four wheels, with an 80% front and 20% rear distribution.

The actual vehicle test and simulation results are compared between the measured and calculated lateral acceleration values at each part, as shown in Figures 11~13. From Figures 11~13, it can be seen that the simulation results agree reasonably well with the measurements, in terms of time-domain and frequency domain, respectively.

In Figure 11 (c), the frequency spectrum of the tie-rod that is near the disc brake is relatively concentrated on 15 Hz. In Figure 12 (c), the frequency spectrum of the rack-housing, which is the Gear-box, is relatively concentrated on 1~2 Hz. In Figure 13 (c), the frequency spectrum of the steering wheel is relatively concentrated on 15 and 40 Hz. Though the frequency range appears beween 0 Hz and 40 Hz in the simulation results, the frequency range of the simulation results is similar to that of the test results.

4. OPTIMIZATION

4.1. Sensitivity Analysis

In the sensitivity analysis process, simulations are executed to determine the relatively important design factors, which is significantly advantageous in saving costs and resources. Sensitivity analysis is performed, based on the suspension parameters using the Plackett-Burman design table. The objective function for the analysis is defined as the RMS value of the steering wheel acceleration. Also, the analysis is implemented in a two-level factor experiment, as shown in Table 3.

The design variables (DV1~DV6) are placed in the front suspension, as shown in Figure 4. Based on each design variable, simulation is performed eight times. As a result, the estimated response function is presented to the sensitive level of each part. The descending order of the design variables regarding sensitivity analysis is DV4 > DV3 > DV1 > DV6 > DV2 > DV5, as shown in Figure 14.

The optimal design will be implemented using the top four variables in terms of sensitivity analysis, namely, DV1, DV3, DV4, and DV6.

Table 4. Design variables.

Factor (Design variable)			Level		
			-1	0	+1
Hardness of G-bush (HS)		DV1	60	65	70
Hardness of Rack-housing MTG. Bush (HS)		DV3	70	80	90
Hardness of A-bush (HS)		DV4	65	70	75
Damper Characteristic (kNs/m)	Extension	DV6	1.49	1.65	1.82
	Compression		0.74	0.82	0.90

Table 5. Experimetal table and results.

No.	DV1	DV3	DV4	DV6	Result (mm/s^2)
1	-1	-1	-1	-1	3647.04
2	-1	-1	-1	1	4214.09
3	-1	-1	1	-1	3377.55
4	-1	-1	1	1	3197.29
5	-1	1	-1	-1	3351.69
6	-1	1	-1	1	3787.10
7	-1	1	1	-1	3367.68
8	-1	1	1	1	3144.66
9	1	1	1	1	3670.40
10	1	1	1	-1	3752.88
11	1	1	-1	1	3365.58
12	1	1	-1	-1	3391.41
13	1	-1	1	1	3661.68
14	1	-1	1	-1	3758.09
15	1	-1	-1	1	3527.54
16	1	-1	-1	-1	3596.51
17	0	0	0	0	3238.86
18	-1.414	0	0	0	3899.43
19	1.414	0	0	0	3645.31
20	0	-1.414	0	0	3280.71
21	0	1.414	0	0	3069.52
22	0	0	-1.414	0	3200.76
23	0	0	1.414	0	3147.10
24	0	0	0	-1.414	3217.85
25	0	0	0	1.414	3161.41

4.2. Response Surface Analysis

In this study, based on an experimental design using the response surface analysis method, an optimization process is proposed to minimize judder vibration of the transfer system (Jung *et al*., 2009). If a three-level design variable has four factors, as shown in Table 4, analysis is performed 25 times according to the central composite design table: the analysis results are shown in Table 5. Using the results of the analysis, the regression model function of the measured acceleration function is estimated as Equation (16).

The table of ANOVA (Analysis of Variance) is shown in Table 6, to verify the estimated regression model function. The value of F_0 is greater than the value of F (0.01). So, the estimated model function has to be reliable in the 99% confidence range. Therefore, the estimated model function represents the relationship between the design variables and the characteristic values.

Table 6. Analysis of varation (ANOVA) table.

Factor	S	Φ	V	F_0	F(0.01)
Regression variation	1.88e+6	4	4.70e+5	39.3	4.43
Residual variation	2.39e+5	20	1.19e+4		
Sum	2.12e+6	24			

Table 7. Results of optimization.

Factor		Current value	Final value
Hardness of G-bush (HS)		65	65
Hardness of Rack-housing MTG. bush (HS)		80	82
Hardness of A-bush (HS)		70	65
Damper Characteristic (kNs/m)	Extension	1.65	1.76
	Compression	0.82	0.88
RMS value of acceleration (mm/s^2)		3238.86	3026.32 (6.6%↓)

4.3. Optimization

In this study, the SQP (Sequential Quadratic Programming) method (Vanderplaats, 1984) is applied for optimization.

$$y = 3120+13.9(DV1)-72.4(DV3)-37.2(DV4)+12.3(DV6) +340(DV1^2)+41.7(DV3^2)-8.9(DV4^2)+49(DV6^2) +26.3(DV1)(DV3)+64.4(DV3)(DV4)-93.1(DV4)(DV6) +180(DV1)(DV4)-7.3(DV3)(DV6)-54.6(DV1)(DV6) \quad (16)$$

When the objective function uses a second-order, nonlinear polynomial, SQP can find the optimal design variables regarding the objective function. Through sensitivity analysis, the bush stiffness and damper characteristic are used as the design variables. Table 5 shows the optimization results. After the optimization process, the bush and damper characteristics are changed. The steering wheel acceleration is reduced. According to the optimized judder test results, the RMS value of the acceleration is decreased by 6.6% (3238.86 $mm/s^2 \rightarrow$ 3026.32 mm/s^2) compared to the test results for the current design variables, as shown in Table 7.

5. CONCLUSION

In this paper, in order to analyze transferred judder phenomena, the bush and damper model are considered as a non-linearity and damping. Also, the rack-pinion gear clearance is expressed as a numerical model. Judder pathways are analyzed for the influence of vibration during

braking, through driving analysis.

The established analytical model is compared with an actual vehicle test. Also, this model can be used to analyze the judder pathway. Suspension connected parts are optimized by using response surface analysis for vibration reduction in the judder pathway. Various design parameters are selected, such as the bush characteristic, mounting angle, damper characteristic, and spring characteristic. Also, the RMS value of the lateral acceleration at the steering wheel is chosen as the objective function. Based on the optimized judder test results, the RMS value of the acceleration is decreased by 6.6% relative to the test results, using the current design variables. The optimization process can be used to select the proper design variables for reducing transfer system vibration using the analyzed numerical model. In the future, in order to improve the accuracy of the analysis results, the brake mechanical motion will be developed in detail.

REFERENCES

Choi, B. K., Park, J. H. and Ahn, B. J. (2007). Development of the virtual test technology for evaluating thermal performance of disc brake. *Spring Conf. Proc. Korean Society of Automotive Engineers*, 659–666.

Cho, K. S. (2008). Viscoelastic measurement and structure of polymeric material. *Trans. Polymer Science and Technology* **19**, **2**, 170–176.

Dixon, J. C. (1999). *The Shock Absorber Handbook*. SAE. 249–278. USA.

Haigh, M. J., Smales, M. and Abe, M. (1993). Vehicle judder under dynamic braking caused by disc thickness variation. *Proc. Institution Mechanical Engineers*, *Paper No.* C444/022.

Hwang, I. J. and Park, G. J. (2005). System mode and sensitivity analysis for brake judder reduction. *Trans. Korean Society of Automotive Engineers* **13**, **6**, 142–153.

Ikhouance, F., Maòosa, V. and Rodellar, J. (2007). Dynamic properties of the hysteretic bouc-wen model. *Int. J. Systems and Control Letters*, **56**, 197–205.

Jung, S. P., Park, T. W., Jun, K. J. and Yoon, J. W. (2009). A study on the optimization method for a multi-body system. *Int. J. Mechanical Science and Technology*, **23**, 950–953.

Kalantari, R. and Foomani, M. S. (2009). Backlash nonlinearity modeling and adaptive controller design for an electromechanical power transmission system. *Trans. B: Mechnical Engineering* **16**, **6**, 463–469.

Kim, H. S., Kim, C. B. and Yim, H. J. (2003). Quality improvement for brake judder using design for six sigma with response surface method and sigma based robust design. *Int. J. Automotive Technology* **4**, **4**, 193–201.

Kim, S. H., Han, E. J., Kang, S. W. and Cho, S. S. (2008). Investigation of influence factors of a brake corner system to reduce brake torque variation. *Int. J. Automotive Technology* **9**, **2**, 233–247.

Meyer, R. (2005). Brake judder – Analysis of the excitation and transmission mechanism within the coupled system brake, chassi and steering system. *SAE Paper No.* 2005-01-3916.

Ok, J. K., Lee, S. K., Yoo, W. S., Sohn, J. H. and Park, S. J. (2005). Bushing model for vehicle dynamcis analysis using Bouc-Wen hysteretic model. *Proc. DETC*, *No*. 84379.

Pevec, M., Potrc, I., Bombek, G. and Vranesevic, D. (2012). Prediction of the cooling factors of a vehicle brake disc and its influence on the results of a thermal numerical simulation. *Int. J. Automotive Technology* **13**, **5**, 725–733.

Shin, D. C., Kim, T. J., Chi, T. S. and Kim, K. Y. (2000). Optimal brake disc design method for high speed judder reduction. *Fall Conf. Proc. Korean Society of Automotive Engineers*, 905–912.

Singh, A. and Lukianov, G. (2007). Simulation process to investigate suspension sensitivity to brake judder. *SAE Paper No.* 2007-01-0590.

Vanderplaats, G. N. (1984). *Numerical Optimization Techniques for Engineering Design*. McGraw-Hill. USA. 195–201.

Voros, J. (2010). Identification of cascade systems with backlash. *Int. J. Control* **83**, **6**, 1117–1124.

Vries, A. and Wagner, M. (1992). The brake judder phenomenon. *SAE Paper No.* 920554.

Zhang, L., Ning, G. and Yu, Z. (2007). Brake judder induced steering wheel vibration: Experiment, simulation and analysis. *SAE Paper No.* 2007-01-3966.